Proceedings of the 9th U.S. National and 10th Canadian Conference on Earthquake Engineering
Compte Rendu de la 9ième Conférence Nationale Américaine et
10ième Conférence Canadienne de Génie Parasismique
July 25-29, 2010, Toronto, Ontario, Canada • Paper No 778

CYCLIC EVOLUTION OF DAMAGE AND BEAM-COLUMN INTERACTION STRENGTH OF CONCRETE-FILLED STEEL TUBE BEAM-COLUMNS

Mark D. Denavit[1], Jerome F. Hajjar[2], Tiziano Perea[3] and Roberto. T. Leon[4]

ABSTRACT

The assessment of response of composite seismic force resisting systems requires accurate nonlinear formulations for the composite members. In this work, reporting the first phase of a NEES project, a three-dimensional distributed plasticity formulation is presented for both circular and rectangular composite concrete-filled steel tubes (CFTs) that includes new constitutive models for the concrete and steel materials to enable tracking of the critical cyclic response of CFTs, including confinement of the concrete core leading to concrete cracking and crushing, and cyclic local buckling of the steel tube. The formulation is validated against an extensive series of new experiments of full-scale circular and rectangular concrete-filled steel tube beam-columns that were tested cyclically under three-dimensional loading (compression plus biaxial flexure). The loading histories to which the specimens were subjected were chosen to catalog the beam-column interaction strength, to document the evolution of damage to CFTs subjected to different types of cyclic loading histories, and to explore the evolution of the stress-resultant loading surface (i.e., the beam-column interaction strength surface) under cyclic loading. Experimental observations of the evolution of the loading surface indicate a change in position and shape as well as a significant decrease in size of the beam-column strength surface under high levels of inelastic loading. This paper addresses the comparison between the computational formulation and experimental results and discusses the implications of the experimental findings on nonlinear modeling of composite seismic force resisting systems.

Introduction

Composite columns have been shown to have high strength, stiffness, and ductility. However, little data is available to justify the structural system response factors (e.g., R, C_d, and Ω_o) given in the specifications. In addition, there are significant gaps in the test data particularly related to slender, full-scale composite beam-columns. In the current work, we strive to fill these

[1] Graduate Research Assistant, Dept. of Civil Engineering, University of Illinois at Urbana-Champaign, IL 61801
[2] Professor, Dept. of Civil Engineering, University of Illinois at Urbana-Champaign, IL 61801
[3] Graduate Research Assistant, Dept. of Civil Engineering, Georgia Institute of Technology, Atlanta, GA 30332
[4] Professor, Dept. of Civil Engineering, Georgia Institute of Technology, Atlanta, GA 30332

gaps through developing system response factors; assessing beam-column strength; and establishing guidelines for the computation of equivalent composite beam-column rigidity to be used in seismic analysis and design of composite frames. Accurate nonlinear static and dynamic computational formulations are required to achieve these goals. Specifically, for developing rational system response factors, a model should directly simulate all predominate inelastic effects from the onset of yielding through strength and stiffness degradation causing collapse, while being sufficiently robust to track inelastic force redistribution without convergence problems up to the point of collapse (FEMA 2009).

Finite Element Formulation

Three-Dimensional Mixed Beam-Column Element

Frame analyses using distributed-plasticity beam-column elements strike a favorable balance of computational efficiency and accuracy. Additionally, mixed formulations (defined here as treating both element displacements and stress resultants as primary state variables) allow for accurate modeling of both geometric and material nonlinearities. Tort and Hajjar (2007) developed a three-dimensional mixed beam-column element for the analysis of composite frames that include rectangular concrete-filled steel tube members, validating against a large number of experimental tests of composite members and frames. This finite element was adapted and further validated against an additional set of experimental tests on circular concrete-filled steel tube members (Denavit 2009). The element stiffness and internal force was derived in the corotational frame, allowing rigid body modes of deformation to be accounted for solely in a geometric transformation. Due to the nature of the mixed formulation two additional equations beyond element equilibrium, element compatibility and section equilibrium must be satisfied. This adds to the complexity of the state determination algorithm. The unbalance from these equations is converted to an unbalanced force at the global level and eliminated through the global solution iterations. Implemented within the OpenSees framework (OpenSees 2009), the element can be used with the wide variety of other elements and solution algorithms available in the framework.

Uniaxial Cyclic Constitutive Relations for CFT Members

The formulation relies on accurate constitutive relations to achieve accurate results. Several uniaxial constitutive relations have been proposed for concrete-filled steel tube (CFT) members (e.g., Susantha et al. 2001; Sakino et al. 2004; Tort and Hajjar 2007; Denavit 2009). Typically, the relations are unique to the shape of the steel tube (e.g., rectangular or circular) because of differences in behavior, namely different confinement of the concrete core, effects of residual stresses on the stress-strain response, and behavior of local buckling of the steel tube. Each of these models uses different assumptions and methods of calibration, but they generally strive to mimic the response of concentrically loaded short CFT columns. The analyses presented in this paper make use of constitutive relations based primarily on the work of Tort and Hajjar (2007) and Denavit (2009).

The constitutive relation for the concrete core is adapted from the rule-based model of Chang and Mander (1994). The tensile branch and the cyclic rules were used without changes. However, the compressive branch was altered to reflect the state of confinement existing in CFT

members. As described in Tort and Hajjar (2007) for rectangular CFTs (RCFT) and Denavit (2009) for circular CFTs (CCFT), sets of well-documented experiments on concentrically load short columns were selected for calibration of the constitutive relations. These tests were selected to have combinations of high and low values of steel yield stress, F_y, concrete compressive strength, f'_c, and ratio of steel tube diameter or depth the thickness, D/t ratio.

The level of confinement experienced by the concrete has a significant impact on the behavior of CFT members. For circular members the confinement serves to increase both the strength and ductility of the concrete core, whereas, for rectangular members only the ductility is affected. The compressive backbone stress-strain curve for the concrete is based on the model of Tsai (Chang and Mander 1994), which is defined by the initial slope E_c, peak coordinate (ε'_{cc}, f'_{cc}), and r factor. The initial slope and strain at peak stress for unconfined concrete, ε'_c, are defined using expressions from the literature (Eqs. (1) and (2), Chang and Mander 1994). The peak stress and strain at peak stress are taken as the unconfined values for RCFT members, whereas for CCFT members they are computed using a confinement model [Eqs. (3) and (4) (Chang and Mander 1994)] and estimation of the confinement pressure (f_l, Eq. (5), Denavit 2009). The r factor, which controls the nonlinear descending branch, was calibrated to the post-peak behavior of short concentrically loaded CFT columns, and also differs between CCFTs and RCFTs (Eq. (7)).

$$E_c\left[\text{MPa}\right] = 12,400 + 500 f'_c\left[\text{MPa}\right] \tag{1}$$

$$\varepsilon_c = f'_c\left[\text{MPa}\right]^{1/4} \Big/ 28 \tag{2}$$

$$f'_{cc} = f'_c\left(-1.254 + 2.254\sqrt{1 + 7.94\left(f_l / f'_c\right)} - 2.0\left(f_l / f'_c\right)\right) \tag{3}$$

$$\varepsilon'_{cc} = \varepsilon_c\left(1 + 5\left(f'_{cc} / f'_c - 1\right)\right) \tag{4}$$

$$f_l = \alpha_\theta F_y \frac{2}{D/t - 2} \tag{5}$$

$$\alpha_\theta = -0.138 + 0.00174\left(D/t\right) \tag{6}$$

$$r = \begin{cases} 0.4 + 0.016\left(D/t\right)\left(f'_c / F_y\right) & \text{for CCFT} \\ 0.3 + 0.11\left(D/t\right)\left(f'_c / F_y\right) & \text{for RCFT} \end{cases} \tag{7}$$

The steel model is based on the bounding-surface plasticity model of Shen et al. (1995). Several modifications were made to model the behavior of cold formed steel tubes. First, to model the built-in residual stress from cold-forming, an initial plastic strain of 0.0006 for CCFT members and 0.0006 and 0.0004 for the corner and flat regions, respectively, of RCFT members is assumed, these values were obtained through comparisons with tensile coupon tests of cold-formed steel tubes (Tort and Hajjar 2007; Denavit 2009). Second, for CCFT members, the backstress of the initial yield surface was shifted to account for the presence of the hoop stresses described by Eq. (6). Additional modifications were made to model local buckling. Local buckling is assumed to initiate when a certain critical strain, ε_{lb} (Eq. (8)), based on results of concentrically loaded short columns where the initiation of local buckling is explicitly indicated, has been reached. For strains higher than the local buckling strain, the response is assumed to be a linear descending branch followed by a constant residual stress branch. The slope of the linear descending branch, K_s (Eq. (9)) is based on a slenderness parameter, R (Eq. (11)), for RCFT

members. The constant residual stress, F_{res} (Eqs. (10)), is based on the stress at the occurrence of local buckling, F_{lb}, and a slenderness parameter, R (Eq. (11)). The residual stress and descending slope were both calibrated to obtain correspondence to the sets of well-documented concentrically loaded short CFT column experiments discussed above.

$$\varepsilon_{lb} = \begin{cases} \left(F_y/E_s\right)\left(0.214R^{-1.41}\right) & \text{for CCFT} \\ \left(F_y/E_s\right)\left(3.14\left(\frac{D}{t}\sqrt{\frac{f_y}{E_s}}\right)^{-1.48}\right) & \text{for RCFT} \end{cases} \tag{8}$$

$$K_s = \begin{cases} -E_s/30 & \text{for CCFT} \\ \min\left[0, -3.22E_s(R-0.08)\right] & \text{for RCFT} \end{cases} \tag{9}$$

$$F_{res} = \begin{cases} \max\left[F_{lb}, 0.17F_{lb}/R\right] & \text{for CCFT} \\ \max\left[F_{lb}, 0.16-0.73RF_{lb}\right] & \text{for RCFT} \end{cases} \tag{10}$$

$$R = \left(D/t\right)\left(F_y/E_s\right) \tag{11}$$

To validate the models, a large number of comparative analyses were performed. Sets of experimental data grouped by loading type were assembled. The loading types include: concentrically loaded short column (additional to the calibration sets), bending, proportionally loaded beam-columns, non-proportionally loaded beam-columns, and cyclic. Figure 1 shows three representative samples of the validation studies. The cyclic RCFT test subjected a beam-column to a constant axial load and cyclically increasing displacements to cause double-curvature. The proportionally loaded test subjected a beam-column to eccentric axial load with an identical eccentricity at each end. The cyclic CCFT test subjected the beam to cyclic equal moments at each end. In each of these cases, strong agreement is seen between the experimental and analytical results.

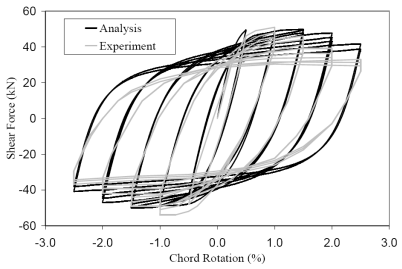

Cyclically Loaded RCFT Beam-Column; Sakino and Tomii 1981; Specimen CIIS3-3; F_y = 298 MPa; f'_c = 27.0 MPa; D/t = 23.8; L/D = 6.0; P/P_o = 0.30

(a)

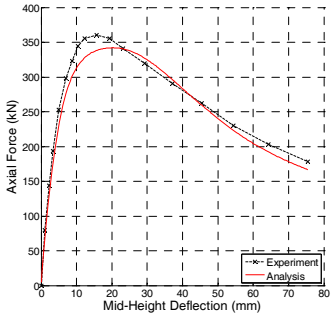

Proportionally Loaded CCFT Beam-Column; Kilpatrick and Rangan 1999; Specimen SC-9; F_y = 410 MPa; f'_c = 58 MPa; D/t = 42.4; L/D = 19.1; $ecc./D$ = 0.098

(b)

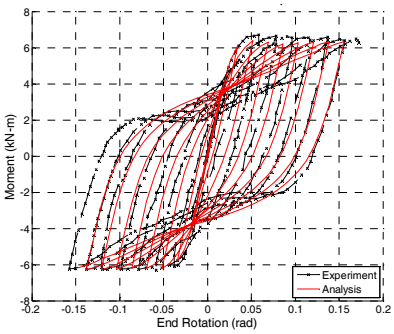

Cyclically Loaded CCFT Beam; Elchalakani and Zhao 2008; Specimen F04I1; F_y = 430 MPa; f'_c = 23.1 MPa; D/t = 88.3; L/D = 7.25

(c)

Figure 1. Representative Model Validation Results

Full-Scale CFT Beam-Column Tests

A series of full-scale concrete-filled steel tube (CFT) beam-column tests has been conducted at the NEES MAST Laboratory at the University of Minnesota. The specimens were selected to fill gaps in prior experimental research, namely to have high member slenderness and high section slenderness (*D/t* ratio). Parameters in the experimental study include: section shape and size, member length, concrete strength. A full description of the testing program is presented in a companion paper (Perea et al. 2010).

The specimens were fixed at the base and for the majority of the testing the specimens were controlled so as to approximate a free boundary condition at the top. The load protocol of each specimen is divided into several load cases. The first load case subjects the specimen to concentric load, the second and third load cases subject the specimen to constant axial load and cyclic transverse displacements, causing uniaxial flexure, the fourth set of load cases subjects the specimen to biaxial flexure plus axial compression. The specific pattern of biaxial flexure varied among the eighteen specimens. As an example, one specimen, RS-18-12, was subjected to a series of "probes" and "subprobes" in its latter load cases. After the completion of the first three load cases, the specimen was moved to zero displacement and a compressive axial load of 3,560 kN (800 kips), which was held constant for the remainder of the test, was applied. A probe was completed by increasing the lateral displacements with a fixed ratio of X to Y displacement until a desired displacement, generally past the limit surface, was reached (stability was maintained because the lateral degrees-of-freedom were in displacement control). From this position a series of subprobes were completed by increasing the displacements in a different fixed ratio of X to Y displacement until the critical flexural strength was reached, at which point the lateral displacements were reversed to the termination point of the original probe. The process was then repeated for several additional X/Y displacement combinations. Assuming that relatively little damage is sustained during the motion of the subprobes, this scan about the termination point of the probe determines the new limit surface of the beam-column. The process was repeated several times, with load cases 4 through 9 representing six distinct probe/subprobe sets. The lateral displacement history is seen in Figure 2. An analogous motion was performed in section analyses for the investigation of the evolution of limit surfaces in steel wide-flange cross sections (Hajjar 2003).

Experimental and Analytical Results: Specimen RS-18-12

The material and geometric properties of specimen RS-18-12 are shown in Table 1. For load cases 1 through 3, the specimen was tested in the strong axis, holding the displacement in the weak axis direction constant at zero. Two cycles of concentric load were applied to the specimen in load case 1. The critical load of the column exceeded the capacity of the MAST system, so these cycles were performed between zero and the capacity of the MAST system (5,900 kN). These amounted to elastic cycles and the experimental results are not shown. Load cases 2 and 3 were performed at 5,340 kN and 1,780 kN respectively. Two full cycles of lateral displacement were applied. Experimental results are shown in Figure 3.

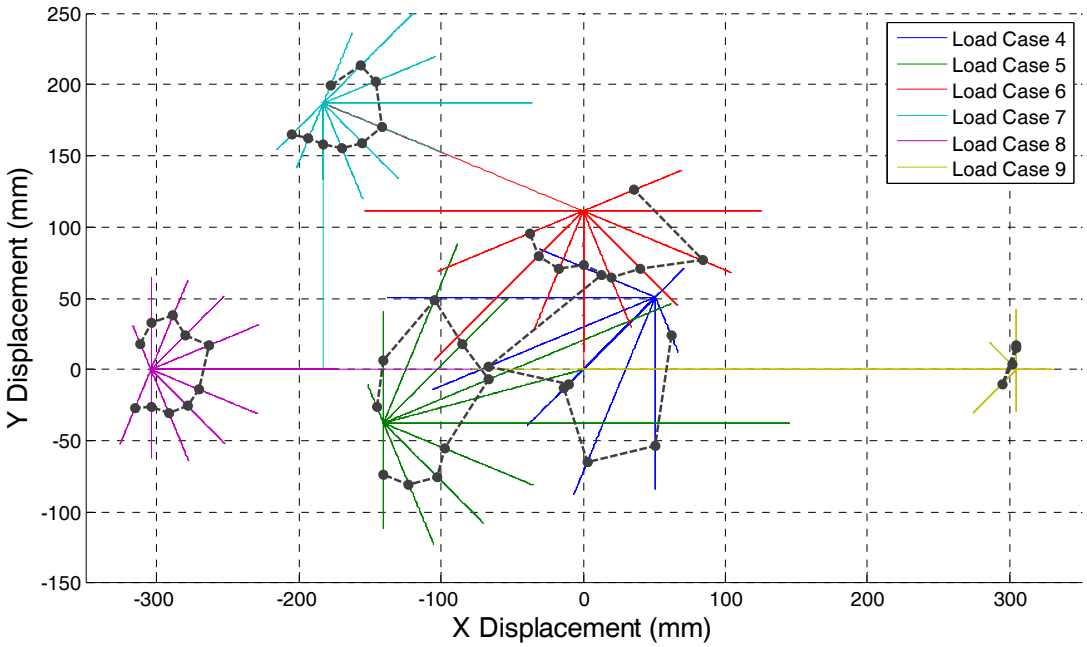

Figure 2. Displacement of the beam-column top, Specimen RS-18-12

Table 1. Geometric and Material Properties of Specimen RS-18-12

Property	**Measured Value**
Column Length, L	5,553 mm
Steel Tube Depth, D	508 mm
Steel Tube Width, B	305 mm
Steel Tube Thickness, t	7.15 mm
Steel Yield Stress, F_y	397 MPa
Steel Ultimate Stress, F_u	521 MPa
Steel Modulus of Elasticity, E_s	202,000 MPa
Concrete Compressive Strength, f'_c	91.7 MPa
Initial Out-Of-Plumbness	X Dir: 20 mm; Y Dir: -6 mm

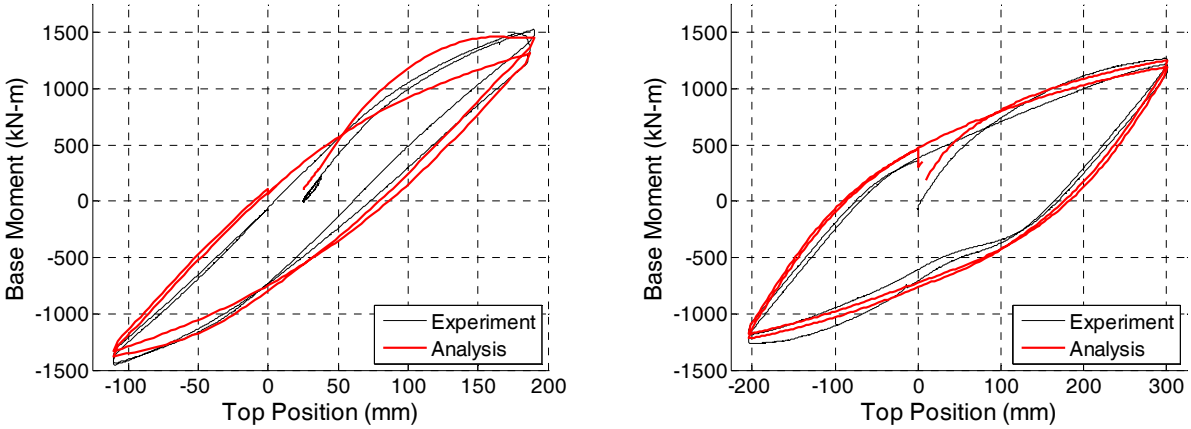

(a) Load Case 2 (b) Load Case 3

Figure 3. Experimental and analytical results of load cases 2 and 3 for specimen RS-18-12

The latter load cases, 4 though 9, were probe/subprobe sets as described above. Where possible, a limit point was identified for each subprobe. The limit point was defined as when the slope in a plot of displacement vs. force of either the X or Y direction was approximately equal to zero, indicating incipient instability due to combined material and geometric nonlinearity due to flexure plus axial compression. These points are shown in Figure 2 as black dots. Connecting the limit points from the various subprobes creates experimental interaction surfaces in lateral displacement space. Using the same limit points, corresponding experimental interaction surfaces can be created in bending moment at the base space (Figure 4). These represent a slice of the three-dimensional (P-$M_{x,base}$-$M_{y,base}$) interaction surface for the applied axial load.

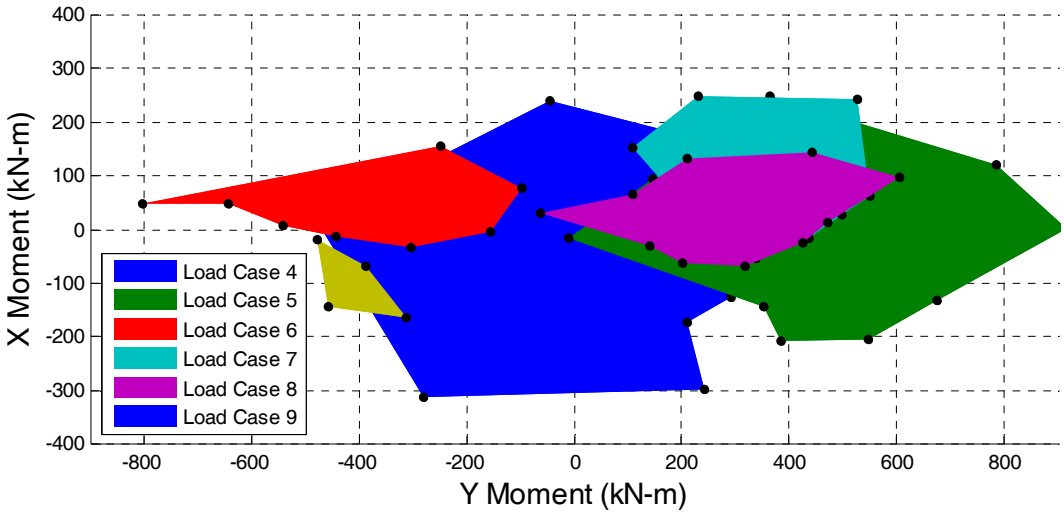

Figure 4. Experimental interaction surfaces

From Figure 2 and Figure 4 it can be seen that the position, shape, and size of the limit surface evolve throughout the loading history. The shape of the interaction surfaces is approximate; however, an oblong trend is seen, with larger Y bending moments corresponding to the strong axis of the specimen and smaller X moments corresponding to the weak axis of the specimen. By comparing the relative locations of the load cases in both Figure 2 and Figure 4, the position of the interaction surfaces appears to be affected by the position of the termination point of the probe. Also, it can be seen that the size of the interaction surfaces decreases as the loading progresses. However, as the load cases progressed the distance between the termination point of the probe to the center location became greater, so it is unclear whether it is damage from cyclic loading or another factor that is diminishing the size of the interaction surface. The inelastic buckling limit state which defines these interaction surfaces is affected by a combination of material and geometric nonlinearity. As such, a wide variety of factors will influence the behavior, including material strengths and section properties at the section level, to beam-column length and out-of-plumbness at the member level.

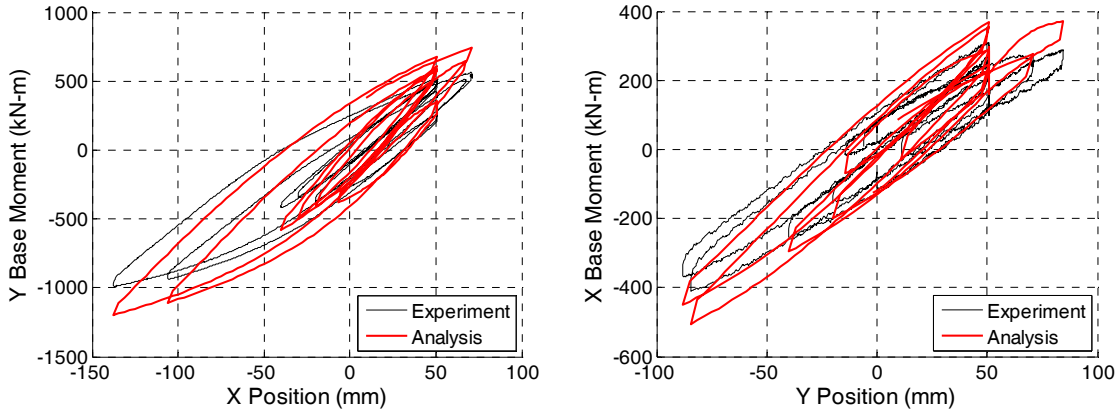

(a) Load Case 4

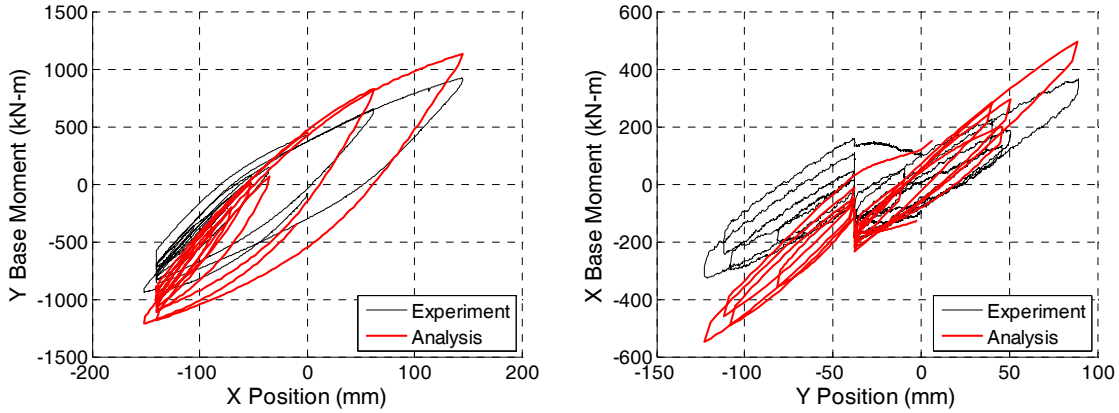

(b) Load Case 5

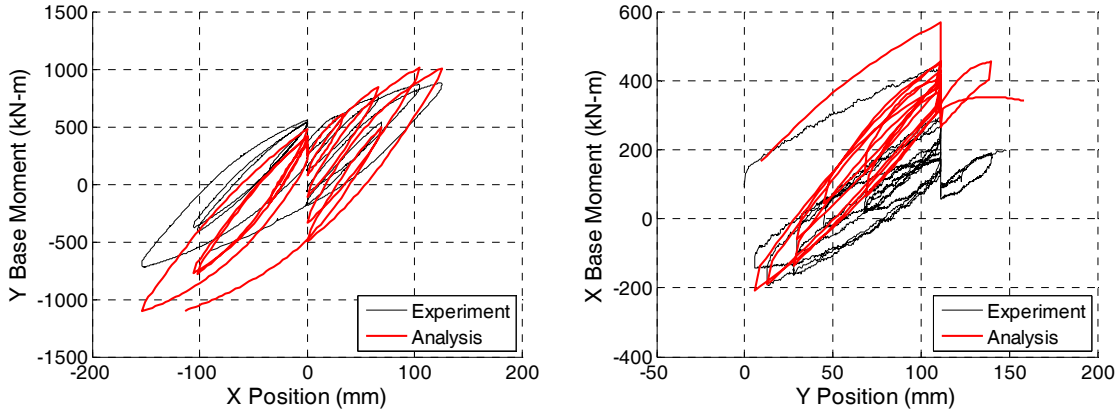

(c) Load Case 6

Figure 5. Experimental and analytical results of load cases 4, 5, and 6 for specimen RS-18-12

Using the finite element formulation, comparable results were attained. A model was created using measured material and geometric properties (Table 1). Four elements with three integration points each were used along the length of the beam-column. The beam-column was modeled as initially straight but with the measured initial out-of-plumbness. Friction in MAST system was modeled using zero length springs at the top of the column. The constitutive model associated with the zero length springs was modeled a stiff modulus up to a slip force of 4.4 kN,

determined from observations of the experimental data, after which the spring modulus was set to zero. The loading history of all nine load cases was applied in sequence. Since there was a negligible amount of inelasticity in load case 1, as noted above, the result are not shown. The results from load cases 2 and 3 are shown in Figure 3. The computational results compare well to the experimental results for both load cases, peak moments, as well as, initial and softening slopes correspond well. Experimental and computational results from load cases 4, 5, and 6 are shown in Figure 5. The correspondence between the results for these load cases is less than for the previous load cases, owing to the difficulty of nonlinear three-dimensional analyses. However, a reasonable comparison is attained.

These results provide an indication that a fiber-based distributed plasticity beam-column formulation, such as the one presented here, is capable of modeling the complex behavior of CFT members subjected to large three-dimensional cyclic loading, including capturing the evolution of the limit surface.

Conclusions

A finite element formulation for analysis of CFT members and frames has been presented. The formulation included a mixed based distributed-plasticity beam element and uniaxial constitutive relations developed for rectangular and circular CFT members. The uniaxial constitutive relations account for the salient features of CFT behavior including confinement of the concrete core and local buckling of the steel tube. The finite element formulation thus provides an accurate analysis tool for use with composite frames.

A series of experiments on full-scale CFT beam-columns has been completed. The tests explore several aspects of the behavior of composite columns, including the multi-dimensional interaction surface, biaxial cyclic seismic behavior, and evolution of damage. The experimental results of one specimen were examined in detail as an example of this investigation. Through a series of probes and subprobes, experimental interaction surfaces were created. These surfaces were shown to evolve in size, position, and shape as the loading progressed. Corresponding computational results were presented, which showed a good correspondence with the experimental results, indicating that the finite element formulation is capable of predicting the complex behavior observed in CFT members.

Acknowledgments

The work described here is part of a NEESR project supported by the National Science Foundation under Grant No. CMMI-0619047, the American Institute of Steel Construction, the Georgia Institute of Technology, and the University of Illinois at Urbana-Champaign. In-kind funding was provided by Atlas Tube Inc. and LeJeune Steel Co. The valuable group effort of the MAST Personnel to the experimental program is greatly appreciated. Any opinions, findings, and conclusions expressed in this material are those of the authors and do not necessarily reflect the views of the National Science Foundation or other sponsors.

References

Chang, G. A. and J. B Mander, 1994. Seismic Energy Based Fatigue Damage Analysis of Bridge Columns: Part I - Evaluation of Seismic Capacity, *Technical Report NCEER-94-0006*, National

Center for Earthquake Engineering Research, State University of New York at Buffalo, Department of Civil Engineering, Buffalo, New York.

Denavit, M., 2009. Nonlinear seismic analysis of circular concrete-filled steel tube members and frames, *M.S. Thesis*, University of Illinois at Urbana-Champaign.

Elchalakani, M. and X.-L. Zhao, 2008. "Concrete-filled cold-formed circular steel tubes subjected to variable amplitude cyclic pure bending," *Engineering Structures*, 30(2), 287-299.

FEMA, 2009. Quantification of Building Seismic Performance Factors, *FEMA P695*, Federal Emergency Management Agency, Washington, D.C.

Hajjar, J. F, 2003. "Evolution of stress-resultant loading and ultimate strength surfaces in cyclic plasticity of steel wide-flange cross-sections," *Journal of Constructional Steel Research*, 59, 713-750.

Kilpatrick, A. E. and B. V. Rangan, 1999. "tests on high-strength concrete-filled steel tubular columns," *ACI Structural Journal*, 96(2), 268-274.

OpenSees, 2009. *Open System for Earthquake Engineering Simulation*, Open source software, http://opensees.berkeley.edu.

Perea, T., R. T. Leon, M. D. Denavit, and J. F. Hajjar, 2010. Experimental tests on cyclic beam-column interaction strength of concrete-filled steel tubes, *Proceedings of the 9th US National and 10th Canadian Conference on Earthquake Engineering*. Toronto, Canada.

Sakino, K., H. Nakahara, S. Morino, and I. Nishiyama, 2004. "Behavior of centrally loaded concrete-filled steel-tube short columns," *Journal of Structural Engineering*, 130(2), 180-188.

Sakino, K. and M. Tomii, 1981. "Hysteretic behavior of concrete filled square steel tubular beam-columns failed in flexure," *Transactions of the Japan Concrete Institute*, 3, 439-446.

Shen, C., I. H. P. Mamaghani, E. Mizuno, and T. Usami, 1995, "Cyclic behavior of structural steels. II: theory," *Journal of Engineering Mechanics*, 121(11), 1165-1172.

Susantha, K. A. S., H. Ge, and T. Usami, 2001. "Uniaxial stress–strain relationship of concrete confined by various shaped steel tubes," *Engineering Structures*, 23(10), 1331-1347.

Tort, C. and J. F. Hajjar, 2007. Reliability-Based Performance-Based Design of Rectangular Concrete-Filled Steel Tube (RCFT) Members and Frames, *Structural Engineering Report No. ST-07-1*, Department of Civil Engineering, University of Minnesota, Minneapolis, Minnesota, August.